Earth and Planetary Science Letters 369-370 (2013) 284–293

Contents lists available at SciVerse ScienceDirect

Earth and Planetary Science Letters

journal homepage: www.elsevier.com/locate/epsl

Large-scale fluctuations in Precambrian atmospheric and oceanic oxygen levels from the record of U in shales

C.A. Partin [a,*], A. Bekker [a], N.J. Planavsky [b], C.T. Scott [c], B.C. Gill [d], C. Li [e], V. Podkovyrov [f], A. Maslov [g], K.O. Konhauser [h], S.V. Lalonde [i], G.D. Love [j], S.W. Poulton [k], T.W. Lyons [j]

[a] Department of Geological Sciences, University of Manitoba, Winnipeg, Manitoba, Canada R3T 2N2
[b] Division of Earth and Planetary Sciences, Caltech, Pasadena, CA 91106, USA
[c] Department of Earth and Planetary Sciences, McGill University, Montreal, QC, Canada H3A 2A7
[d] Department of Geosciences, Virginia Polytechnic Institute, Blacksburg, VA 24061, USA
[e] State Key Laboratory of Biogeology and Environmental Geology, China University of Geosciences, Wuhan 430074, China
[f] Institute of Precambrian Geology and Geochronology, Russian Academy of Sciences, St. Petersburg, Russia
[g] Zavaritskii Institute of Geology and Geochemistry, Urals Branch, Russian Academy of Sciences, Ekaterinburg, Russia
[h] Department of Earth and Atmospheric Sciences, University of Alberta, Edmonton, AB, Canada T6G 2E3
[i] European Institute for Marine Studies, 10 UMR 6538 Domaines Océaniques, Technopôle Brest-Iroise, 29280 Plouzané, France
[j] Department of Earth Sciences, University of California, Riverside, CA, 92521, USA
[k] School of Earth and Environment, University of Leeds, Leeds LS2 9JT, UK

ARTICLE INFO

Article history:
Received 17 July 2012
Received in revised form
17 March 2013
Accepted 23 March 2013
Editor: G. Henderson
Available online 25 April 2013

Keywords:
Precambrian
rise of atmospheric oxygen
ocean
atmosphere
uranium in the ocean

ABSTRACT

The atmosphere–ocean system experienced a progressive change from anoxic to more oxidizing conditions through time. This oxidation is traditionally envisaged to have occurred as two stepwise increases in atmospheric oxygen at the beginning and end of the Proterozoic Eon. Here, we present a study of the redox-sensitive element, uranium, in organic-rich shales to track the history of Earth's surface oxidation at an unprecedented temporal resolution. Fluctuations in the degree of uranium enrichment in organic-rich shales suggest that the initial rise of atmospheric oxygen ~2.4 billion yr ago was followed by a decline to less oxidizing conditions during the mid-Proterozoic. This redox state persisted for almost 1 billion yr, ending with a second oxygenation event in the latest Neoproterozoic. The U record tracks major fluctuations in surface oxygen level and challenges conventional models that suggest the Earth underwent a unidirectional rise in atmospheric oxygen during the Precambrian.

© 2013 Elsevier B.V. All rights reserved.

1. Introduction

Numerous lines of evidence indicate very low levels of atmospheric oxygen on the early Earth (Holland, 2006). The common occurrence of detrital uraninite, siderite, and pyrite, as well as the presence of mass-independent sulfur isotope fractionation in sedimentary rocks, indicate very low levels of atmospheric oxygen ($<10^{-5}$ of present atmospheric level, PAL) prior to the Great Oxidation Event (GOE; Holland, 2006) at ~2.4 Ga (Bekker et al., 2004). The beginning of the GOE is marked by the onset of terrestrial pyrite oxidation (e.g. Canfield, 1998; Canfield and Raiswell, 1999; Konhauser et al., 2011), the disappearance of detrital redox-sensitive minerals from the sedimentary record (Roscoe and Minter, 1993), and the first appearance of red beds, which all indicate the operation of oxidative processes in terrestrial environments (Holland, 1984). As a result, the continental flux of dissolved uranium and redox-sensitive chalcophilic/siderophilic elements to the oceans should have increased dramatically after the GOE with the advent of strong oxidative continental weathering (Holland, 1984). However, these proxies collectively provide only a rough lower estimate on atmospheric oxygen after the GOE (~1–10% PAL) (Holland, 2006). The upper limit suggested for the mid-Proterozoic (1.8–0.8 Ga) is based on evidence for widespread ocean anoxia (<40% PAL) (Canfield, 2005), though the temporal and geographic extent and nature of the anoxia has been difficult to estimate, in part due to the incomplete nature of the mid-Proterozoic geologic record and available proxies. By the late Neoproterozoic, atmospheric oxygen level increased again, where the lower estimate is ~15% PAL (Canfield et al., 2007). Phanerozoic oxygen levels are typically thought to have fluctuated between ~70% and 170% PAL (Berner, 2009), but it is very likely that O_2 levels were lower than 20–60% PAL during the early Paleozoic (e.g., Bergman et al., 2004). Therefore, the Phanerozoic (the last ~540 million yr) was characterized by a dynamic, but generally well-oxygenated atmosphere–ocean system relative to the

* Corresponding author.
E-mail address: umpartin@cc.umanitoba.ca (C.A. Partin).

0012-821X/$ - see front matter © 2013 Elsevier B.V. All rights reserved.
http://dx.doi.org/10.1016/j.epsl.2013.03.031

Precambrian. Since the redox state of the Earth's oceans and atmosphere are linked, anoxia is generally thought to have been more prevalent in Proterozoic oceans under low atmospheric oxygen levels (Wilde, 1987; Canfield, 1998). Therefore, the redox state of the oceans in the past provides insight into atmospheric as well as seawater oxygen levels (Canfield, 1998, 2005).

The GOE has been envisioned to be a permanent oxidation event that started between 2.45 and 2.32 Ga (Bekker et al., 2004) and continued for 200 million yr (Holland, 2002). After the initial rise of atmospheric oxygen, recorded by the loss of the mass-independent fractionation in sulfur isotopes and the loss of detrital redox-sensitive minerals (Bekker et al., 2004), progressive oxygenation of the atmosphere and oceans was sustained by an event of high organic carbon burial, called the Lomagundi Event, which is recorded by highly positive carbon isotope values in marine carbonates deposited between ~2.22 and 2.06 Ga (8‰ and higher, Karhu and Holland, 1996). Conservative estimates for oxygen release coupled to increased organic carbon burial during the Lomagundi Event range from 12 to 22 times the present atmospheric inventory (Karhu and Holland, 1996). However, some of this oxygen released over the ~140 million yr-long Lomagundi Event was consumed by oxidation of the upper continental crust and oceans (Kump et al., 2011; Bekker and Holland, 2012).

The dissolved concentrations of redox-sensitive elements (e.g., Mo, V, and U) in the oceans directly reflect the average global seawater oxidation state (Emerson and Huested, 1991), since the residence time of these elements is longer than the typical oceanic mixing time (1–2 kyr). This relationship is underpinned by the premise that the burial rates of many redox-sensitive elements (e.g., Mo, V, Re, Cr, and U) are much higher in anoxic and low-oxygen water columns as compared to those in well-oxygenated settings (Emerson and Huested, 1991; Algeo, 2004; Tribovillard et al., 2006). Mo, for example, is the most abundant transition element in the ocean today (with a seawater concentration of ~105 nM), despite its scarcity in the continental crust (~1 ppm). This is a direct result of the modern marine redox state; euxinic (anoxic and sulfidic) and suboxic sediments with sulfidic pore waters (environments where Mo is preferentially buried) are extremely spatially limited, allowing Mo to accumulate to its present level in seawater (e.g., Emerson and Huested, 1991; Scott et al., 2008). Therefore, the smaller the extent of reducing conditions in the ocean, the larger the marine reservoir of Mo (Emerson and Huested, 1991; Hastings et al., 1996; Algeo, 2004; Tribovillard et al., 2006).

Uranium is preferentially buried in sediments underlying low-oxygen and anoxic (both sulphidic and ferruginous, unlike Mo) water columns (Anderson et al., 1989; Klinkhammer and Palmer, 1991; Dunk et al., 2002), making it a reliable proxy to track the extent of diverse reducing conditions. Uranium is also one of the few elements not sourced from hydrothermal systems (German and von Damm, 2003). Therefore, U has strong potential among the redox-sensitive elements to track the dynamics of Earth's surface oxygenation, and can provide further constraints complementary to those obtained from the Mo record (Scott et al., 2008). Given the source–sink control on the reservoir size of trace elements, we can use the secular variations in marine redox-sensitive element concentrations (inferred from the sedimentary record) to refine our understanding of oxygen dynamics during and after the GOE.

We present herein U concentrations from over 2700 shale samples spanning most of Earth's history, from geographically separated areas covering every continent (except Antarctica). Paleoproterozoic and Archean units are from a diverse set of cratons, including the Kapvaal and Congo cratons (Africa), Pilbara and Yilgarn cratons (Australia), Superior craton (Canada), Dharwar craton (India), Karelia and Kola cratons (Northern Europe/Russia), and the North China craton (China); see Table S2 for detailed geological setting of each sampled unit. Data from marine shales were filtered to include only units of greenschist or lower metamorphic grade in order to prevent potential bias due to post-depositional alteration. Importantly, we used conventional redox proxies, Fe/Al ratios (Lyons et al., 2009) and iron speciation data (Raiswell et al., 2001; Poulton and Raiswell, 2002), to screen for samples deposited under locally anoxic (either sulphidic or ferruginous) water column conditions. For each sample presented in our compilation there is independent evidence for deposition under anoxic conditions. Given that all of the shales in the database were deposited under anoxic conditions, each had the potential for U enrichment during deposition. Sedimentary U enrichment (i.e., authigenic U sequestration) in these samples will therefore mirror the size of the marine U reservoir, although local depositional controls (e.g., sedimentation rate and organic matter loading) will also exert a control on magnitude of U enrichment in sediments. Given this framework, our coupling of proxies can help us gauge shifts in sources and sinks for U in the ocean and the evolution of the marine U reservoir through time.

With the end goal of providing new insights into how oxygen levels in the atmosphere–ocean system changed through time, we describe the modern marine U cycle, discuss the significance of secular variations in the U content of shales based on our dataset, and use a simple mass balance model to explore the ancient marine U cycle.

2. The modern marine U cycle

Uranium has two distinct geochemical states, oxidized and soluble U(VI) and reduced and immobile U(IV) (Langmuir, 1978). Oxidative continental weathering is required to solubilize U(VI) from continental crust, which has an average uranium content of 2.7 ppm (Taylor and McLennan, 1985). Subsequently, rivers deliver dissolved U as soluble hexavalent U(VI) to the ocean. Riverine delivery represents the only significant source of U to the oceans today, with an average riverine concentration of 1.2 nM (Dunk et al., 2002). This flux, however, would have varied in the past with the strength of chemical weathering linked to atmospheric oxygen level and climate (see Section 4.1—the ancient marine U cycle). U is conservative in modern oxic seawater; the present seawater [*U*] is 14 nM (~3.3 ppb, Ku et al., 1977). U(VI) is the most stable U valence state under oxic conditions (Langmuir, 1978), and is the dominant U species in oxic seawater today (Tribovillard et al., 2006), even under anoxic marine water columns, such as in the Black Sea (Anderson et al., 1989), and usually forms strong complexes with bicarbonate, such as uranyl tetracarbonate ($UO_2(CO_3)_3^{4-}$) (Langmuir, 1978).

The burial of U in anoxic marine sediments is the largest U sink in the modern ocean. Under reducing marine conditions, U(VI) is reduced to the immobile tetravalent state (U(IV)) and sequestered primarily into organic-rich shales (Anderson et al., 1989), possibly as fine-grained uraninite (UO_2) (Klinkhammer and Palmer, 1991). Notably, the U content of organic-rich sediments roughly tracks organic matter content (Klinkhammer and Palmer, 1991; Dunk et al., 2002; Tribovillard et al., 2006).

The concentration of U in seawater is controlled largely by the extent of reducing conditions within the ocean (Emerson and Huested, 1991; Klinkhammer and Palmer, 1991; Dunk et al., 2002). Today, suboxic ('low-oxygen') and anoxic continental margin sediments constitute approximately 55–80% of the U sink (Barnes and Cochran, 1990; Klinkhammer and Palmer, 1991; Dunk et al., 2002). "Suboxic" sediments refer here to sediments with O_2 penetration depth <1 cm, following the definition used by Dunk et al. (2002); this is generally consistent with the

definition used by Barnes and Cochran (1990) for sediments undergoing nitrate reduction. Within this sink, sediments deposited beneath fully anoxic waters account for a substantial portion of the overall U sink (~27–40% of the riverine flux, Dunk et al., 2002), despite their extremely limited spatial distribution (< 0.5% of the seafloor). The rate at which U is sequestered into anoxic sediments is ~14 × higher than in suboxic sediments. The average calculated by Dunk et al. (2002) for a variety of modern anoxic settings (~219 μg U cm^{-2} kyr^{-1}) is close to our average based on literature data (251 μg U cm^{-2} kyr^{-1}; see Supplementary materials). Suboxic sediments sequester U at a much lower rate on average (17 μg U cm^{-2} kyr^{-1}; Dunk et al., 2002), and might be affected by post-depositional oxygenation (Zheng et al., 2002). Since suboxic sediments cover a much larger area of the seafloor today relative to anoxic sediments, this accounts for a roughly similar proportion of the total U sink. A lesser proportion of U is incorporated into biogenic carbonates (mostly in calcareous invertebrates) and silica and removed from the ocean, accounting for ~13–32% and 0.5–2% of riverine delivery (Dunk et al., 2002). Additionally, U(VI) is scavenged during submarine weathering of basalt via adsorption onto iron oxyhydroxides, which could potentially account for 6–20% of oceanic uranium sink (Hsi and Langmuir, 1985; Dunk et al., 2002).

Both biotic and abiotic mechanisms may be important for U(VI) reduction (Hsi and Langmuir, 1985; Lovley et al., 1991; Lovley and Phillips, 1992; Barnes and Cochran, 1993; Behrends and Van Cappellen, 2005). Uranium that diffuses into anoxic or suboxic sediments precipitates biologically by means of either metal-reducing bacteria or their byproducts (e.g., sulfide) or non-biologically by sorption onto organic matter or iron oxides (Hsi and Langmuir, 1985; Zheng et al., 2002). The dominant mechanism of U reduction might be microbially-mediated as Fe (III)- and sulfate-reducing bacteria have been shown in laboratory experiments to reduce U(VI) to U(IV) to obtain energy (Lovley and Phillips, 1992; Barnes and Cochran, 1993; Behrends and Van Cappellen, 2005). Anderson et al. (1989) observed that U occurs almost exclusively in the soluble oxidized U(VI) state in the Black Sea's anoxic water column, suggesting that U(VI) is not reduced even under the high levels of H_2S in the water column. Conversely, data from Van der Weijden et al. (1990) suggest that in sulfidic oceanic waters with a relatively long residence time (> 1000 yr), U reduction is kinetically favorable. This is still a slow process (< 30% reduction in dissolved seawater U(VI) content over 1000 yr), and is not likely to have contributed to a significant portion of the U sink in past oceans.

The rate of U removal from anoxic bottom waters into anoxic sediments appears to directly vary with respect to dissolved U concentration (Barnes and Cochran, 1993; Zheng et al., 2002), allowing us to assume that anoxic sediment uranium content (U_{sed}) reflect — to a first approximation — dissolved marine uranium concentrations (U_{sw}) when normalized to the organic flux (Algeo and Lyons, 2006). Maximum values of U_{sed} in anoxic sediments thus provide insights into the upper limit for U_{sw} in seawater, as U_{sed} is limited by U_{sw} at any given time (Emerson and Huested, 1991; Algeo, 2004; Algeo and Maynard, 2008). Assuming a constant riverine U flux after the GOE, and because the size of the marine U reservoir was directly tied to the extent of anoxic and low-oxygen conditions, it is possible to track the evolution of the oceanic U reservoir and ocean ventilation via the magnitude of U_{sed} in organic-rich, anoxic shales.

We present a modern U budget based on average published rates for the major marine U sinks in an ocean set to be in steady-state with the annual riverine U input (Table 1). From this framework, we used a simple sensitivity model to explore the past U marine cycle. We explore changes in the ancient marine U cycle (Section 4.1), largely by varying the extent of ocean anoxia. The general disappearance of detrital uraninite, even in rapidly accumulated sediments, after ~2.2 Ga (e.g., Grandstaff, 1980; Holland, 1984) suggests that atmospheric oxygen level after that time was sufficiently high to oxidize exposed uraninite (> ~1% PAL). It implies that the global riverine U flux after that time was essentially decoupled from atmospheric oxygen partial pressure. Consequently, in our sensitivity model we have assumed a modern riverine U flux to the Proterozoic oceans.

3. Analytical methods

New major and trace element data for this study was generated by inductively-coupled mass-spectrometry (ICP-MS) at University of California, Riverside, Arizona State University, Activation Labs, ACME Labs, and by x-ray fluorescence (XRF) and ICP-MS at the Zavaritskii Institute of Geology and Geochemistry, Uralian Branch of the Russian Academy of Sciences, Ekaterinburg, Russia using matrix-matched calibration standards, dominantly USGS SDO-1 and SGR1b. Based on duplicate analyses of geostandards, error of Fe, Al, U, and Th was better than 5% for ICP-MS data and 10% for XRF data. Data assembled from the literature was generated with a wide range of techniques including ICP-MS, ICP-OES, and XRF. Reproducibility for literature data is estimated to be better than ~90%. Total organic carbon was determined based on the difference between total carbon and the inorganic carbon contents using an Eltra CS-500 carbon–sulfur analyzer at University of California, Riverside and University of Manitoba, utilizing B2150 and USGS SGR1b for total carbon calibration and as quality control standards, and AR1034 (calcite) standard for total inorganic carbon calibration. Reproducibility is 0.1% for total organic carbon analyses. The data were passed through several screens including relatively low metamorphic grade (greenschist-facies or lower), high organic carbon content (> 0.4%), and well-established age constraints on deposition. As mentioned above, since only the content of U in sediments deposited under anoxic marine conditions track the budget of U in the oceans, we imposed filters on our compiled dataset to select anoxic shales (Fig. 1). Data were subject to a Fe/Al ratio filter, where shales with Fe/Al ratio greater than 0.5 (average crustal value, Taylor and McLennan, 1985) are assumed to represent anoxic depositional conditions (cf. Lyons and Severmann, 2006), though higher thresholds (e.g., Fe/Al > 0.6) do not change the overall trend. In the absence of major element data in some datasets, other parameters indicating anoxic settings (e.g., degree of pyritization) were used and therefore these data were also included in Fig. 1 (see Supplementary database). The iron speciation paleoredox proxies are reviewed in detail elsewhere (Lyons and Severmann, 2006; Poulton and Canfield, 2011).

4. Results and discussion

Our compilation of U_{sed} in organic-rich shales from ~3.2 Ga to the present (Fig. 1) fits well into four distinct stages, reflecting changes in the marine U cycle that occurred in direct response to the evolution of oceanic and atmospheric oxygen levels. When normalized to total organic carbon content (Fig. 2), the data trend is comparable to that delineated by authigenic U content, suggesting that U_{sed} content reflects the size of the local and perhaps global marine U reservoir, rather than temporal variations in U scavenging associated with changes in organic matter burial. Our discussion stems mainly from the U_{sed} enrichment plot (Fig. 1), since it has a higher density of data points than the U/TOC plot (Fig. 2), especially in key intervals.

Table 1
Modern oceanic U budget. Anoxic and suboxic organic-rich sediments are the largest marine U sink. Anoxic sediments are those overlain by an anoxic water column or anoxic bottom waters (e.g., Black Sea, Cariaco Basin; ~0.3–0.5% of seafloor); suboxic sediments are those with oxygen penetration depth of <1 cm and are confined to oxygen-minimum zone and partially-silled basins such as the California Borderland basins (4–6% of seafloor; Morford and Emerson, 1999). Rates for U sequestration into altered basalts and biogenic carbonates are from Dunk et al. (2002) and are given in μg U/kyr. Anoxic and suboxic organic-rich sediments account for ~69% of riverine flux in our modern U budget.

Sink	Suboxic sediments	Anoxic sediments	Altered basalt	Biogenic carbonate	Residence time
Average burial rate (μg U cm^{-2} kyr^{-1}) and [area of seafloor]	17 [5%]	251 [0.5%]	–	–	~400 kyr
Total burial flux (μg U kyr^{-1} × 10^{18})	2.98	4.39	1.39	1.81	
% of Riverine U flux	~35–60%	~27–42%	~6–20%	~13–32%	

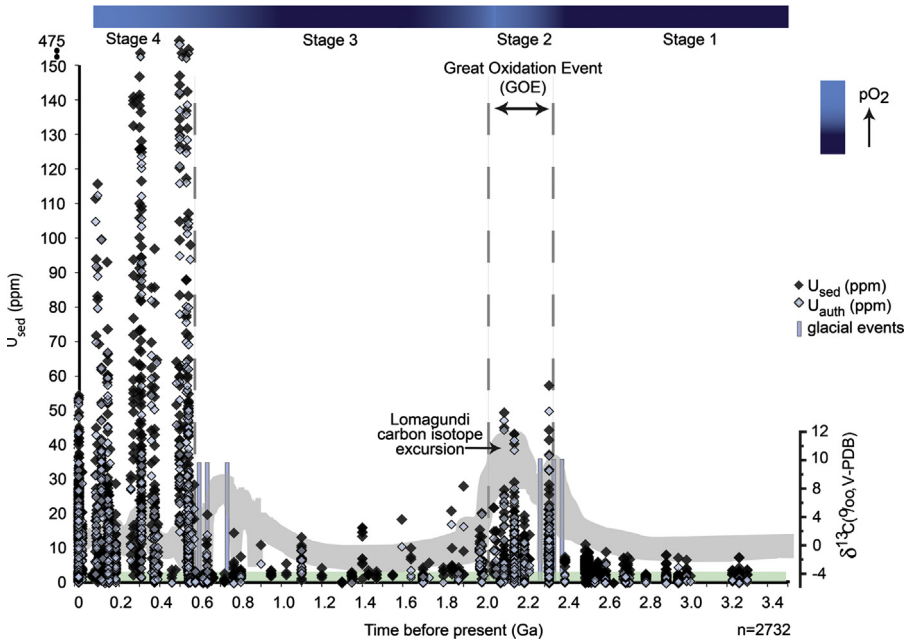

Fig. 1. U_{sed} content and authigenic enrichments ($U_{auth}=U_{total}$–Th/3, Wignall and Myers, 1988) in organic-rich shales through time. Green bar at the base of the figure indicates average continental crust value (2.7 ppm, Taylor and McLennan, 1985). The U shale record suggests that the redox history of the Precambrian atmosphere–ocean system is characterized by both increases and decreases in atmospheric oxygen level linked to the burial of organic carbon, as shown by the secular variation in carbon isotope composition of carbonates (gray band, modified from Karhu (1999)). (For interpretation of the references to color in this figure legend, the reader is referred to the web version of this article.)

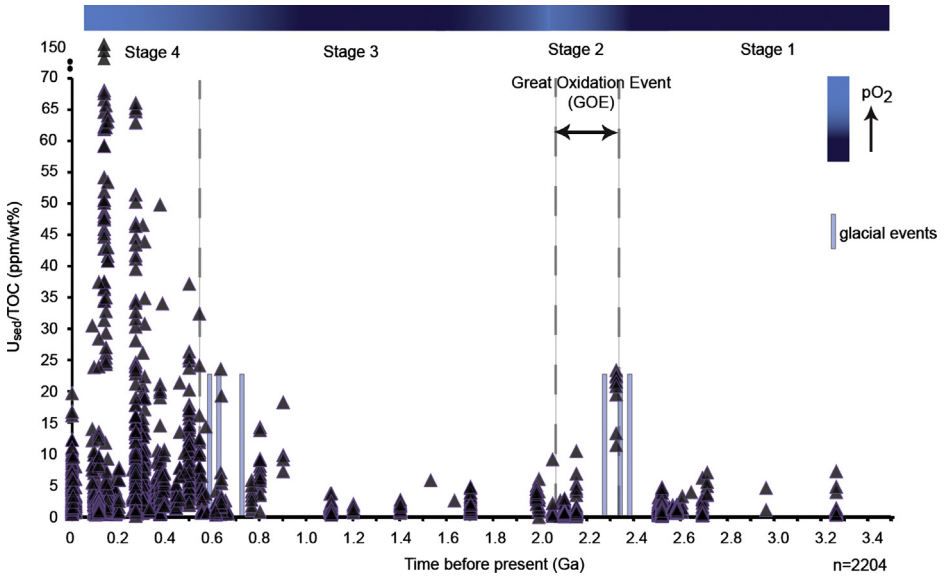

Fig. 2. U_{sed} content normalized to TOC in organic-rich shales with greater than 0.4 wt% TOC.

Stage 1 encompasses the Archean and earliest Paleoproterozoic (>2.32 Ga)—the interval before the rise of atmospheric oxygen. The end of this stage coincides with glaciations linked with the rise of atmospheric oxygen (Bekker et al., 2004; Barley et al., 2005). The lack of significant U enrichment (U content <10 ppm, average ~3.8 ppm) in organic-rich shales deposited prior to ~2.32 Ga points to a low concentration of soluble U in terrestrial and marine waters due to anoxic surface conditions. This interpretation is consistent with the presence of detrital uraninite, pyrite, and siderite in fluvial and shallow-marine conglomerates and sandstones older than ~2.4 Ga (Roscoe and Minter, 1993; Rasmussen and Buick, 1999), which are interpreted to indicate anoxic atmospheric conditions on the early Earth (Holland, 2006).

While the chemical composition of the upper continental crust has evolved through time (Taylor and McLennan, 1985), the Th/U ratio of the upper continental crust has been essentially constant since 3.5 Ga (Th/U=3.8–4.0, Condie, 1993). Importantly, this eliminates potential variations in the continental source of U to the ocean that would have been otherwise rooted in the evolution of the chemical composition of the upper continental crust (see U_{auth} in Fig. 1). Similarly, secular variations in the U_{sed} record are not likely to be related to the changes in the availability of fresh, unweathered continental crust exhumed during supercontinent cycles, which would be recorded in the Th/U ratios through time. There is a general lack of correlation between the U_{sed} record and assembly and breakup of the known supercontinents, since there are no spikes in the U content of shales during the intervals when weathering and erosion of crust is expected to be the highest, for example, in the aftermath of the ~1.9–1.8 Ga Trans-Hudson orogeny (during Nuna assembly) or ~1.0 Ga Grenville orogeny (during Rodinia assembly). The lack of variation in Th/U ratios since the Archean and the lack of correlation with supercontinent cycles suggest that any variation in riverine delivery of U to the oceans through time is not driven by secular variations in the evolution and production of continental crust. We suggest that riverine delivery of U was roughly constant after the GOE, since the oxidation of the major U-bearing mineral (uraninite) was unlikely to be limited by atmospheric oxygen levels after the end of our stage 1.

Importantly, the secular evolution of U minerals confirms the U_{sed} trend through time. Uranyl (U(VI)) minerals do not appear in the mineralogical record until after the GOE (Hazen et al., 2009), emphasizing the role of the atmosphere-ocean system redox state in the evolution of U-cycling (Fig. 3).

Stage 2 lasted from ~2.32 to ~2.06 Ga and spans the prominent rise of atmospheric oxygen at the GOE, which includes the longest and largest positive carbon isotope excursion in Earth's history, the Lomagundi Event (Karhu and Holland, 1996). The stage starts with a marked increase in U_{sed} content (up to 60 ppm) in organic-rich shales of the ~2.32 Ga Timeball Hill and Rooihoogte formations, South Africa. Several shale units show consistently high U_{sed} content, between 40 and 50 ppm, well above the highest U_{sed} found in shale units deposited during stage 1. The average U_{sed} content in stage 2 shales is 10.7 ppm, demonstrating U enrichments significantly above crustal levels. This prominent change in the U record of organic-rich shales indicates a dramatic transition in the redox state of Earth's atmosphere that led to the onset of strong oxidative continental weathering and the release of U(VI) to fluvial systems, likely for the first time in Earth's history. Though there is some evidence for continental crust oxidation prior to the deposition of these units (e.g., Konhauser et al., 2011), there is not a clear signal for this in the U shale record. Similarly, significant Mo enrichments appear to have formed around 2.5 Ga (Anbar et al., 2007), but continuous oxidation is not demonstrated by the Mo record until ~2.1 Ga (Scott et al., 2008). Short residence times and water column drawdown by scavenging during incipient stages of oxidative riverine supply might explain the lack of obvious and persistent U and Mo enrichments in shales prior to 2.32 Ga. Sustained seawater oxidation during the protracted GOE (our stage 2) is recorded in units of ~2.15 Ga age (e.g., Sengoma and Magaliesberg formations, South Africa, and Ludikovian Series, Russia).

A sharp increase in U_{sed} content at ~2.32 Ga demonstrates a substantial growth in the seawater U reservoir as a direct result of atmospheric and oceanic oxidation. An increase in the U marine reservoir requires that well-oxygenated waters covered a large portion of the continental margins. Generally oxic continental shelves would have inhibited significant U reduction and burial in these settings, in contrast to deposition and efficient U sequestration under an anoxic water column. Mean U_{sed} in Paleoproterozoic shales deposited during stage 2 is approximately 1/5 of the average U enrichment in Phanerozoic shales (Table 2). Consequently, broadly oxic marine conditions, but yet more reducing than those typical of Phanerozoic oceans likely correspond to U data for stage 2. Given the coupling of U burial with organic matter fluxes, the deep ocean plays a relatively small role in the global U cycle. However, since low-oxygen conditions are most likely to develop at mid-water depths (e.g., Paulmier and Ruiz-Pino, 2009), a relatively limited extent of anoxia on continental margins suggests that a large portion of the deep ocean was also ventilated during the Lomagundi Event.

After ~2.06 Ga, during our stage 3, U content in shales shows a remarkable change, returning to near-crustal levels (average of 3.8 ppm), indicating a lack of significant authigenic U enrichment in most of the studied units. This dramatic change in U content of shales could reflect either a decrease in U flux to the oceans, or an increase in the U sink, or potentially both. Constraints on atmospheric oxygen level provided by paleosols (Rye and Holland, 1998; Murakami et al., 2011) and the general absence of detrital redox-sensitive minerals in coarse-grained siliciclastic successions after the GOE (Holland, 1984; Roscoe and Minter, 1993) suggest that the mid-Proterozoic did not experience Archean-like atmospheric oxygen levels. Muted U enrichments in mid-Proterozoic shales are, therefore, attributed to a small marine U reservoir resulting from a long-lived, widespread ocean anoxia. Since the redox state of the ocean is linked to the oxygen content of the atmosphere (e.g., Wilde, 1987; Canfield, 1998), we ascribe the decrease in the U content of shales to a change in atmospheric oxygen content. It should be noted that O_2 solubility in seawater decreases dramatically with an increase in surface temperature. There is no evidence, however, to infer that climate overall during our stage 2 was significantly colder than during stage 3. In this light, U content in mid-Proterozoic shales suggests a fall in the O_2 level of the atmosphere–ocean system after the spike of oxygen associated with burial of organic matter during the Lomagundi Event abated (Kump et al., 2011).

The record of shallow-marine sulfate evaporites, which appeared for the first time at ~2.32 Ga and largely disappeared after ~2.1 Ga (Schröder et al., 2008), provides evidence for a rise and a fall in the size of the marine sulfate reservoir. Oceanic sulfate levels are directly tied to both the oxidation of sulfides on the continents and the oxidation state of the oceans. Sulfur isotope systematics of carbonate-associated sulfate were also recently used to provide evidence for an increase and subsequent decrease in marine sulfate level during our stages 2 and 3 (Planavsky et al., 2012). Therefore, a decrease in the U content of shales driven by ocean oxygenation and deoxygenation is corroborated by a rise and fall in oceanic sulfate level. This emerging view contrasts dramatically with the widely accepted view of an essentially unidirectional or stepwise increase in the oxygen content of the Proterozoic atmosphere–ocean system (e.g., Cloud, 1976; Catling and Claire, 2005; Holland, 2006; Murakami et al., 2011). Our dataset documents both the immediate response of the U cycle

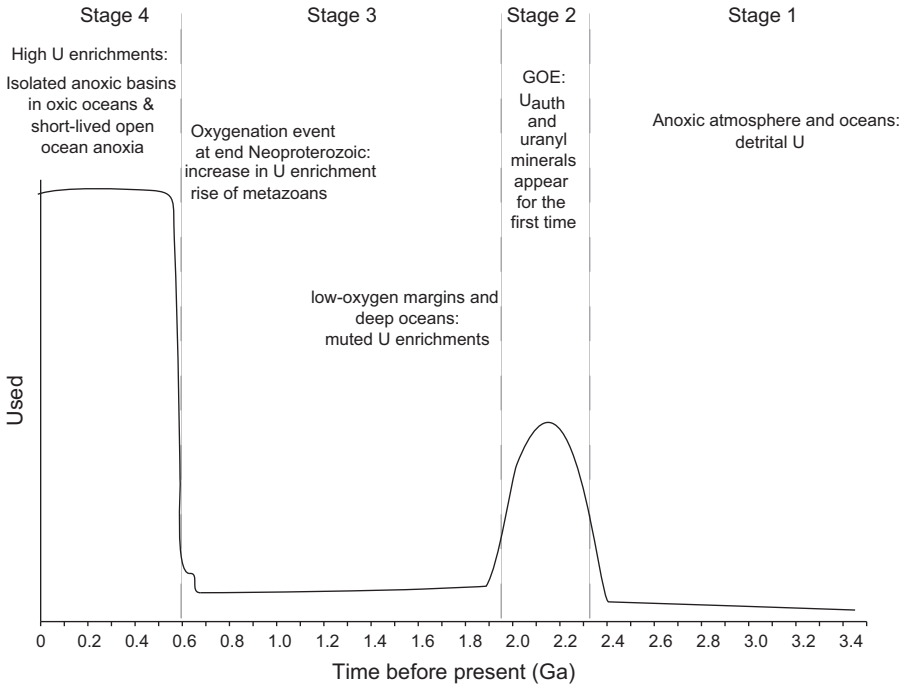

Fig. 3. Summary of U enrichments and implications for the redox state of the atmosphere and oceans in stages as described in the text.

Table 2
Average U_{sed} for anoxic shales in stages 1–4.

	Stage 1	Stage 2	Stage 3	Stage 4
Average U_{sed} (ppm)	3.8, $n=375$	10.7, $n=566$	3.8, $n=324$	26, $n=1566$
Average U/TOC ratio (ppm/wt%)	1.4, $n=290$	2.9, $n=99$	3.0, $n=174$	9.9, $n=1546$
Average U_{auth} (ppm)	0.9, $n=186$	5.1, $n=534$	0.6, $n=298$	24.9, $n=704$

to the rise of atmospheric oxygen and, in contrast to the canonical model, demonstrates subsequent vacillating post-GOE atmospheric and oceanic oxygen levels.

Since we use maximum U enrichment as a proxy for the upper limit of U_{sw} (cf. Emerson and Huested, 1991), it is important to verify that the difference between maximum U_{sed} and U_{sed}/TOC values for stages 2 and 3, which we interpret as a fall in the oxidation state of the atmosphere–ocean system, is statistically significant. To verify that U_{sed} maxima in stages 2 and 3 are distinctly different, we examined the probability of observing values greater than stage 3 maxima in a subsampled population of stage 3 (see Supplementary material). We determined that values of $U_{sed} > 27$ ppm, and $U_{auth} > 18$ ppm will occur in only 0.7% of cases, and U_{sed}/TOC > 16 ppm/weight % will only occur in 1.5% of cases in stage 3. Subsequently, we looked at the number of cases where values would occur above these levels (for U_{sed}, U_{auth}, and U_{sed}/TOC) in both stages 2 and 3, and assessed statistical significance through a chi-squared test. The chi-squared value was larger than the critical value for each variable examined, demonstrating that there are meaningful differences (at the $p < 0.001$ significance level) between stages 2 and 3 in the probability of observing elevated U_{sed} values. This provides a solid justification for a stage boundary between stages 2 and 3 and confirms that shales from stage 3 have the lower maxima level of U_{sed}, which is a first-order estimate for the long-term average concentration of U_{sw} in ancient seawater and the redox state of the atmosphere–ocean system. Our data therefore support sustained lower-oxygen conditions in the atmosphere–ocean system during the mid-Proterozoic, as was previously inferred from iron speciation data for marine shales (Shen et al., 2002, 2003; Poulton et al., 2004, 2010; Planavsky et al., 2011; Poulton and Canfield, 2011).

Further, we highlight that the U enrichments in several anoxic mid-Proterozoic units are similar to those found in the Archean record, suggesting widespread marine anoxia (and very low atmospheric oxygen levels) at least episodically during the Proterozoic. Stated in another way, we should not think of the mid-Proterozoic record collectively. There were likely significant fluctuations in the marine redox state (e.g., Slack et al., 2007; Planavsky et al., 2011) during the mid-Proterozoic and potentially periods with very poorly oxygenated oceans.

Like U contents in shales, carbon isotope variations remained muted for almost a billion years after the Lomagundi Event (Bekker and Holland, 2012), until another organic carbon burial event transpired late in stage 3 prior to Neoproterozoic glacial events (Halverson et al., 2005). A positive carbon isotope excursion and a small increase in maximum U_{sed} content and U_{sed}/TOC ratios in organic-rich shales in the late Neoproterozoic hints at a transition towards a more oxidizing conditions in the atmosphere-ocean system leading up to our stage 4. This assertion is tentative, however, and subsequent work should focus on confirming this earlier oxygenation.

The fourth stage of the Earth's redox evolution started in the late Neoproterozoic and includes all of the Phanerozoic. Stratigraphic and secular trends in U content and high U_{sed} (up to 475 ppm) in organic-rich shales were controlled by short-lived episodes of local to global low-oxygen conditions in the oceans drawing from a large, modern-like seawater U reservoir in association with high organic carbon fluxes. Importantly, persistent and large U enrichments throughout the Phanerozoic indicate a

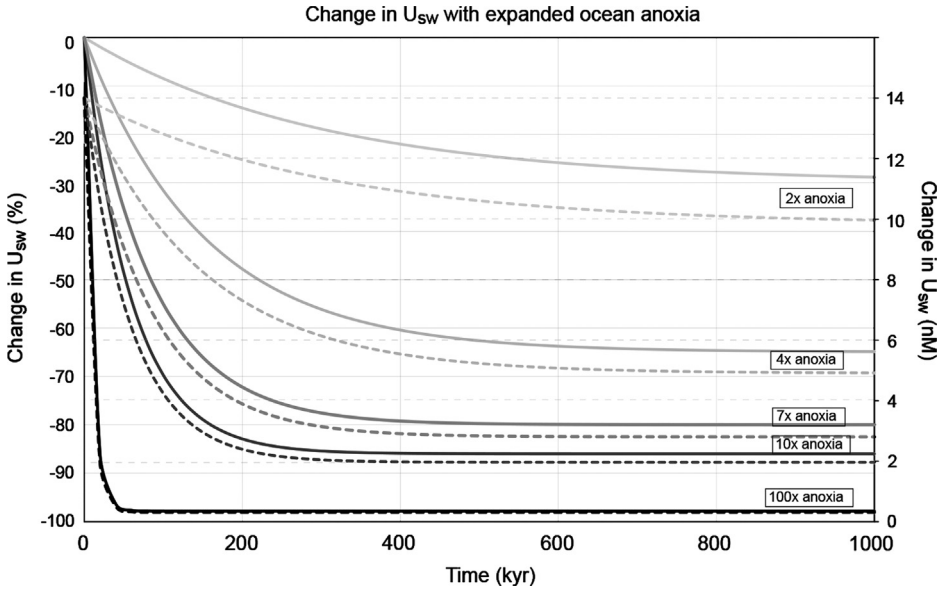

Fig. 4. Sensitivity model for uranium concentration in seawater responding to changes in the area of anoxic seafloor based on a simple oceanic mass balance (after Hastings et al. (1996)). Hypothetical scenarios include increasing anoxia by a factor of 2, 4, 7, 10, and 100 relative to the modern extent of seafloor anoxia. Dashed lines represent the change in U_{sw} in nM, and solid lines represent the % change in U_{sw}. In each scenario, the U_{sw} decreases to a new steady-state concentration over several hundred thousand years. This direct feedback sensitivity model allows us to increase the extent of anoxia, the most important U sink in modern oceans, and achieve a new steady-state U_{sw}. Each sink is directly dependent on seawater U concentration; the three main sinks considered here are the fluxes to anoxic and suboxic sediments (F_a and F_{so}) and to altered seafloor basalts (F_b). These fluxes are calculated based on the following equations: $F_a=\alpha C$, $F_{so}=\beta C$, and $F_b=\varepsilon C$, where C is the concentration of U in seawater and α, β, and ε are calculated based on modern environments. Upon a perturbation to the steady-state system, specifically by increasing the area of anoxia and suboxia, the concentration of U in seawater at time t is given by: $[U]_t=(J_{in}/J_{out})+(U_i-(J_{in}/J_{out}))\exp(-\gamma t)$, where $\gamma=(A_a\alpha+A_{so}\beta+\varepsilon)/Vo$, A_a and A_{so} are the areal extent of anoxic and suboxic sediments, respectively, and Vo is the ocean volume.

fundamentally different marine redox state compared with that of the mid-Proterozoic. The U record shows a transition to a more oxidized ocean by at least the late Neoproterozoic with U_{sed} increasing to values up to 94 ppm by 551 Ma in the upper Doushantuo Formation of South China. This is consistent with the Mo record (Scott et al., 2008), which provides strong evidence for this second major step in atmosphere–ocean oxygenation. Intervals at ~635 Ma and 570 Ma portend this change (Fig. 4) with notable increases above the mid-Proterozoic mean U_{sed} content and U_{sed}/TOC ratios (Figs. 1 and 2) and with U enrichments similar to those found in the modern Cariaco Basin. The 635 Ma and 570 Ma intervals show modern levels of U enrichment in both U_{sed} and U_{sed}/TOC, which is not observed in any of the mid-Proterozoic units (Stage 3). New trace metal (Mo, V, and U) and S isotope data point toward a well-oxygenated atmosphere–ocean system in the aftermath of the 'Snowball Earth' event at ~635 Ma (Sahoo et al., 2012). Therefore, our data corroborate the suggestion that complete and persistent ocean oxidation occurred by at least 551 Ma (Canfield et al., 2007, 2008; Scott et al., 2008), but it also points toward oxygenation in the late Neoproterozoic as early as 635 Ma (cf. Sahoo et al., 2012).

4.1. The ancient marine U cycle

We can estimate the change in seawater residence time of the ancient U cycle relative to the modern by factoring in hypothetical changes in the areal extent of anoxic and suboxic sediments in the ocean, since the majority of riverine input (~55–80%) to the ocean is sequestered into anoxic and suboxic sediments (Klinkhammer and Palmer, 1991; Dunk et al., 2002). We consider only the sinks to suboxic and anoxic sediments, plus the sink to basalts altered by seafloor weathering as relevant to the Precambrian, since biogenic silica and biogenic carbonate production was likely insignificant before the Phanerozoic. To constrain the largest sink in the modern oceanic U budget, we have chosen U burial rates representative of those in modern suboxic and anoxic basins (see Table 1). Our input parameters are broadly consistent with estimates available in the literature for the modern marine U cycle.

Following previous work, we assume a direct relationship between enrichment in redox-sensitive elements in sediments and seawater reservoir size (Emerson and Huested, 1991; Algeo and Maynard, 2008; Scott et al., 2008), which builds from the premise that the level of trace metal enrichment in sediments reflects dissolved seawater concentrations. We construct a simple sensitivity model to understand how change in the extent of anoxia and suboxia in the oceans (i.e., increase in the burial flux of uranium to sediments) would impact oceanic U reservoir size. We assume in our model that burial fluxes directly scale with U_{sw} and the area of the seafloor with anoxic (A_a) or suboxic (A_{so}) conditions, therefore sinks are proportional to the concentration of U in seawater. As such, the first-order relationship is the following:

$$(dC/dt)=J_{in}-J_{out}U_{res} \quad (1)$$

where C is the U concentration in seawater, J_{in} and J_{out} are the source and sink fluxes of U to and from the oceans, respectively, and U_{res} represents the seawater U reservoir, $Vo\cdot C$ (V_o is the volume of the ocean). Specifically, the source and sink fluxes of U in the oceans are described by the following equation (after Hastings et al. (1996)):

$$V_o(dC/dt)=J_R-((A_aR_a)+(A_{so}R_s)+F_b) \quad (2)$$

where J_R is the riverine flux (source), and the sink fluxes (anoxic and suboxic sediments, and submarine basalts) are the second, third, and fourth components on the right side of the equation. Here, A_a and A_{so} are the areas of anoxic and suboxic sediments, respectively; R_a and R_s are the area-specific rates (μg U/cm^2 kyr) at which U is scavenged into anoxic and suboxic sediments, respectively; and F_b is the flux of U to basalts during submarine hydrothermal alteration (directly proportional to U_{sw}).

We look at the change in U_{sw} concentration in a time-integrated framework assuming that riverine flux from the continents did not change significantly after the GOE and was similar

to the modern riverine flux, and that all sink fluxes are directly proportional to U_{sw} (i.e., $F_a=\alpha U_{sw}$, $F_{so}=\beta U_{sw}$, and $F_b=\varepsilon U_{sw}$, where α, β, and ε are calculated to reflect present-day U_{sw}). U_{sw} at time t is described by the following equation:

$$[U_{sw}]_t = (J_{in}/J_{out}) + (U_i - (J_{in}/J_{out}))\exp(-\gamma t) \quad (3)$$

where U_i is the initial U_{sw} before a perturbation of extended anoxia is applied, and $\gamma=(A_a\alpha+A_{so}\beta+\varepsilon)/Vo$. The system typically reaches steady-state in response to a given perturbation on a time scale of 1×10^5–10^6 yr. The oceanic residence time of U is highly sensitive to the surface area of anoxia and suboxia on the ocean floor (Fig. 4). Effectively, our model allows us to estimate the change in the seawater concentration of U after a given increase in anoxic seafloor surface area has been applied and the system has again reached a steady-state.

We calculated oceanic U_{sw} concentrations under several expanded anoxia scenarios (Fig. 4), including doubling the current area of anoxia and increasing it by a factor of 10, using the above described, well-established direct feedback model (Hastings et al., 1996) modified for U that draws from the present understanding of the modern U marine mass balance. These hypothetical scenarios validate the link between expanded anoxia in the ocean and a decreased U seawater reservoir size. That is, in an ocean with expanded anoxia relative to today's oceans, there will be a smaller marine U reservoir, thus the concentration would decrease significantly, similar to the relationship inferred from trace element records of Phanerozoic marine sediments (Algeo, 2004), including Mo (Dahl et al., 2010).

Large increases in the extent of anoxic conditions, relative to today, are needed to substantially decrease the size of the marine U reservoir (Fig. 4). The low U content preserved in Precambrian organic matter-rich shales analyzed in this study (Fig. 1, Table 2) can therefore be linked to an ocean with reducing conditions significantly expanded relative to the modern ocean. Importantly, our estimates of the effect of marine anoxia on U_{sw} are conservative, since we have assumed that all anoxic sediments will have U burial rates typical for near-shore continental margin sediments (Dunk et al., 2002) with high organic carbon and particulate fluxes. Our sensitivity model indicates that only a small area of anoxia on continental margins (3.5–5%) is required to explain the stage 2 record. A seawater U reservoir that is roughly 1/5 of the modern ocean is thus still indicative of a relatively well-oxygenated ocean. Since U reduction rates will decrease with lower organic carbon loading as expected in offshore environments, we have likely underestimated the extent of anoxic conditions ($\sim$50% of the seafloor) needed to decrease the size of the marine U reservoir to the level needed to explain muted authigenic U enrichments in mid-Proterozoic shales ($\sim$2.4% of the average authigenic U enrichment in the Phanerozoic shales, see Table 2). This problem becomes even more acute with lower U enrichments that approach crustal levels. Therefore, we provide only a rough estimate of the possible extent of marine anoxia in the mid-Proterozoic oceans based on the observed muted U enrichments; further work is necessary to elucidate the areal extent of anoxic seafloor in the mid-Proterozoic.

4.2. Implications for atmosphere–biosphere co-evolution

Our results highlight key relations between the oxygenation of the atmosphere–ocean system, organic carbon burial, biological innovations, and climatic events at both ends of the Proterozoic. The Paleoproterozoic GOE is coincident with glaciations and the onset of high burial rates of organic matter that mark the $\sim$140 million yr-long Lomagundi Event. This event was followed by a transition to a long-lived, less-oxidized state of the atmosphere-ocean system. In contrast, Neoproterozoic oxygenation resulted in the eventual establishment of a well-oxygenated steady-state of the atmosphere–ocean system. Though our data agree generally with the notion of a two-step oxygenation of Proterozoic oceans (e.g., Scott et al., 2008), we provide novel evidence for a dramatic, sustained minimum in atmosphere–ocean oxygen levels between these steps. In both the Paleoproterozoic and Neoproterozoic, strong nutrient fluxes (e.g., Planavsky et al., 2010) and supercontinent cycles (Barley et al., 2005; Campbell and Allen, 2008; Campbell and Squire, 2010) were likely important in controlling the onset and dynamics of these events. Biological evolution, however, might be responsible for the final outcome. Surface oxygenation during the Lomagundi Event may have acted as a negative feedback against further atmospheric oxygen rise with greater oxidant availability having a deleterious impact on biological productivity and the burial rate of organic carbon (Kump et al., 2011; Bekker and Holland, 2012). In contrast, Neoproterozoic oxygenation corresponded with the radiation of algae and, finally, metazoans (Butterfield, 2007; Love et al., 2009), resulting in a transition to a biogeochemical carbon cycle approaching that of the Phanerozoic biosphere (Bartley and Kah, 2004). Thus, Neoproterozoic biological innovations (e.g., Butterfield, 2007; Sperling et al., 2007; Tziperman et al., 2011) could have led to more efficient organic carbon export to deep-waters and, consequently, organic carbon burial, resulting in a positive feedback to atmospheric oxygen rise and, ultimately, in the further net oxygenation of the Earth's surface.

5. Conclusions

We have defined four stages in the evolution of the marine U cycle through time. These stages are intimately linked with the evolution of surficial redox conditions. Stage 1 (>2.32 Ga) is characterized by a detrital flux of uranium minerals under low atmospheric O_2 conditions ($<10^{-5}$ PAL). The first increase in the flux of soluble U (U(VI)) accompanied the rise of atmospheric oxygen during the GOE (our stage 2). Stage 2 is characterized by high, modern ocean-like U_{sed} in shales, and demonstrates the growth of a significant oceanic U reservoir relative to that in the Archean. After $\sim$2.06 Ga, the size of the oceanic U reservoir decreased, resulting in low U_{sed} content in shales that are only marginally higher than U_{sed} in stage 1. Considering that the oxygen content of the atmosphere–ocean system directly controls the marine U cycle, we interpret this to reflect a drop in surficial oxidation from stage 2 to stage 3. Stage 4 encompasses the latest Neoproterozoic and all of the Phanerozoic, and is characterized by the highest U values seen in the geologic record. Stage 4 reflects sustained high atmospheric O_2 levels and only transient or isolated anoxia in the Phanerozoic oceans that scavenged U from a large oceanic reservoir in an otherwise well-ventilated ocean.

Acknowledgments

Funding was provided by the NSERC Discovery Grant to A.B.; NSF-EAR Program (Grant EAR-0720362 to T.W.L. and G.D.L.); the NASA Exobiology Program and Astrobiology Institute, and Agouron Institute to T.W.L and G.D.L.; Agouron Institute to B.G.; the Russian Foundation for Basic Research to A.M. and V.P.; AAPG Grants-in-Aid to C.A.P.; NSF-EAR-PDF to N.J.P.; the 973 Program grant and Moe grant of China to C.L. Sharad Master is gratefully acknowledged for providing shale samples from the Mwashya Formation. We thank Tom Algeo and two anonymous reviewers for useful comments that improved the manuscript. The authors dedicate this paper to H.D. Holland.

Appendix A. Supporting information

Supplementary data associated with this article can be found in the online version at http://dx.doi.org/10.1016/j.epsl.2013.03.031.

References

Algeo, T.J., 2004. Can marine anoxic events draw down the trace element inventory of seawater? Geology 32, 1057–1060.

Algeo, T.J., Lyons, T.W., 2006. Mo–total organic carbon covariation in modern anoxic marine environments: implications for analysis of paleoredox and paleohydrographic conditions. Paleoceanography 21, PA1016.

Algeo, T.J., Maynard, J.B., 2008. Trace-metal covariation as a guide to water-mass conditions in ancient anoxic marine environments. Geosphere 4, 872–887.

Anbar, A.D., Duan, Y., Lyons, T.W., Arnold, G.L., Kendall, B., Creaser, R.A., Kaufman, A. J., Gordon, G.W., Scott, C., Garvin, J., Buick, R., 2007. A whiff of oxygen before the Great Oxidation Event? Science 317, 1903–1906.

Anderson, R.F., Fleisher, M.Q., LeHuray, A.P., 1989. Concentration, oxidation state, and particulate flux of uranium in the Black Sea. Geochim. Cosmochim. Acta 53, 2215–2224.

Barley, M.E., Bekker, A., Krapež, B., 2005. Late Archean to Early Paleoproterozoic global tectonics, environmental change and the rise of atmospheric oxygen. Earth Planet. Sci. Lett. 238, 156–171.

Barnes, C.E., Cochran, J.K., 1990. Uranium removal in oceanic sediments and the oceanic U balance. Earth Planet. Sci. Lett. 97, 94–101.

Barnes, C.E., Cochran, J.K., 1993. Uranium geochemistry in estuarine sediments: controls on removal and release processes. Geochim. Cosmochim. Acta 57, 555–569.

Bartley, J.K., Kah, L.C., 2004. Marine carbon reservoir, C_{org}–C_{carb} coupling, and the evolution of the Proterozoic carbon cycle. Geology 32, 129–132.

Behrends, T., Van Cappellen, P., 2005. Competition between enzymatic and abiotic reduction of uranium(VI) under iron reducing conditions. Chem. Geol. 220, 315–327.

Bekker, A., Holland, H.D., 2012. Oxygen overshoot and recovery during the early Paleoproterozoic. Earth Planet. Sci. Lett. 317–318, 295–304.

Bekker, A., Holland, H.D., Wang, P.L., Rumble, D., Stein, H.J., Hannah, J.L., Coetzee, L. L., Beukes, N.J., 2004. Dating the rise of atmospheric oxygen. Nature 427, 117–120.

Bergman, N.M., Lenton, T.M., Watson, A.J., 2004. COPSE: a new model of biogeochemical cycling over Phanerozoic time. Am. J. Sci. 304, 397–437.

Berner, R.A., 2009. Phanerozoic atmospheric oxygen: new results using the Geocarbsulf Model. Am. J. Sci. 309, 603–606.

Butterfield, N.J., 2007. Macroevolution and macroecology through deep time. Palaeontology 50, 41–55.

Campbell, I.H., Allen, C.M., 2008. Formation of supercontinents linked to increases in atmospheric oxygen. Nat. Geosci. 1, 554–558.

Campbell, I.H., Squire, R.J., 2010. The mountains that triggered the Late Neoproterozoic increase in oxygen: the Second Great Oxidation Event. Geochim. Cosmochim. Acta 74, 4187–4206.

Canfield, D.E., 1998. A new model for Proterozoic ocean chemistry. Nature 396, 450–453.

Canfield, D.E., 2005. The early history of atmospheric oxygen: homage to Robert A. Garrels. Annu. Rev. Earth Planet. Sci. 33, 1–36.

Canfield, D.E., Poulton, S.W., Knoll, A.H., Narbonne, G.M., Ross, G., Goldberg, T., Strauss, H., 2008. Ferruginous conditions dominated later Neoproterozoic deep-water chemistry. Science 321, 949–952.

Canfield, D.E., Poulton, S.W., Narbonne, G.M., 2007. Late-Neoproterozoic deep-ocean oxygenation and the rise of animal life. Science 315, 92–95.

Canfield, D.E., Raiswell, R., 1999. The evolution of the sulfur cycle. Am. J. Sci. 299, 697–723.

Catling, D.C., Claire, M.W., 2005. How Earth's atmosphere evolved to an oxic state: a status report. Earth Planet. Sci. Lett. 237, 1–20.

Cloud, P., 1976. Beginnings of biospheric evolution and their biogeochemical consequences. Paleobiology 2, 351–387.

Condie, K.C., 1993. Chemical composition and evolution of the upper continental crust: contrasting results from surface samples and shales. Chem. Geol. 104, 1–37.

Dahl, T.W., Hammarlund, E.U., Anbar, A.D., Bond, D.P.G., Gill, B.C., Gordon, G.W., Knoll, A.H., Nielsen, A.T., Schovsbo, N.H., Canfield, D.E., 2010. Devonian rise in atmospheric oxygen correlated to the radiations of terrestrial plants and large predatory fish. Proc. Natl. Acad. Sci. USA 107, 17911–17915.

Dunk, R.M., Mills, R.A., Jenkins, W.J., 2002. A reevaluation of the oceanic uranium budget for the Holocene. Chem. Geol. 190, 45–67.

Emerson, S.R., Huested, S.S., 1991. Ocean anoxia and the concentrations of molybdenum and vanadium in seawater. Mar. Chem. 34, 177–196.

German, C., von Damm, K., 2003. Hydrothermal processes. In: Elderfield, H. (Ed.), Treatise on Geochemistry: The Oceans and Marine Geochemistry. Elsevier/Pergamon, Oxford, pp. 181–222.

Grandstaff, D.E., 1980. Origin of uraniferous conglomerates at Elliot Lake, Canada and Witwatersrand, South Africa: implications for oxygen in the Precambrian atmosphere. Precambrian Res. 13, 1–26.

Halverson, G.P., Hoffman, P.F., Schrag, D.P., Maloof, A.C., Rice, A.H.N., 2005. Toward a Neoproterozoic composite carbon-isotope record. Geol. Soc. Am. Bull. 117, 1181–1207.

Hastings, D.W., Emerson, S.R., Mix, A.C., 1996. Vanadium in foraminiferal calcite as a tracer for changes in the areal extent of reducing sediments. Paleoceanography 11, 665–678.

Hazen, R.M., Ewing, R.C., Sverjensky, D.A., 2009. Evolution of uranium and thorium minerals. Am. Mineral. 94, 1293–1311.

Holland, H.D., 1984. The Chemical Evolution of the Atmosphere and Oceans. Princeton University Press, Princeton, NJ.

Holland, H.D., 2002. Volcanic gases, black smokers, and the Great Oxidation Event. Geochim. Cosmochim. Acta 66, 3811–3826.

Holland, H.D., 2006. The oxygenation of the atmosphere and oceans. Philos. Trans. R. Soc. London, Ser. B 361, 903–915.

Hsi, C.D., Langmuir, D., 1985. Adsorption of uranyl onto ferric oxyhydroxides: application of the surface complexation site-binding model. Geochim. Cosmochim. Acta 49, 1931–1941.

Karhu, J.A., 1999. Carbon isotopes. In: Marshall, C.P., Fairbridge, R.W. (Eds.), Encyclopedia of Geochemistry. Kluwer Academic Publishers, Boston, pp. 67–72.

Karhu, J.A., Holland, H.D., 1996. Carbon isotopes and the rise of atmospheric oxygen. Geology 24, 867–870.

Klinkhammer, G., Palmer, M., 1991. Uranium in the oceans—where it goes and why. Geochim. Cosmochim. Acta 55, 1799–1806.

Konhauser, K.O., Lalonde, S.V., Planavsky, N.J., Pecoits, E., Lyons, T.W., Mojzsis, S.J., Rouxel, O.J., Barley, M.E., Rosiere, C., Fralick, P.W., Kump, L.R., Bekker, A., 2011. Aerobic bacterial pyrite oxidation and acid rock drainage during the Great Oxidation Event. Nature 478, 369–373.

Ku, T.-L., Knauss, K.G., Mathieu, G.G., 1977. Uranium in open ocean: concentration and isotopic composition. Deep Sea Res. 24, 1005–1017.

Kump, L.R., Junium, C., Arthur, M.A., Brasier, A., Fallick, A., Melezhik, V., Lepland, A., CČrne, A.E., Luo, G., 2011. Isotopic evidence for massive oxidation of organic matter following the Great Oxidation Event. Science 334, 1694–1696.

Langmuir, D., 1978. Uranium solution-mineral equilibria at low temperatures with applications to sedimentary ore deposits. Geochim. Cosmochim. Acta 42, 547–569.

Love, G.D., Grosjean, E., Stalvies, C., Fike, D.A., Grotzinger, J.P., Bradley, A.S., Kelly, A. E., Bhatia, M., Meredith, W., Snape, C.E., Bowring, S.A., Condon, D.J., Summons, R.E., 2009. Fossil steroids record the appearance of Demospongiae during the Cryogenian period. Nature 457, 718–721.

Lovley, D.R., Phillips, E.J., 1992. Reduction of uranium by *Desulfovibrio desulfuricans*. Appl. Environ. Microbiol. 58, 850–856.

Lovley, D.R., Phillips, E.J.P., Gorby, Y.A., Landa, E.R., 1991. Microbial reduction of uranium. Nature 350, 413–416.

Lyons, T.W., Anbar, A., Severmann, S., Scott, C., Gill, B., 2009. Tracking euxinia in the ancient ocean: a multiproxy perspective and Proterozoic case study. Annu. Rev. Earth Planet. Sci. 37, 507–534.

Lyons, T.W., Severmann, S., 2006. A critical look at iron paleoredox proxies: new insights from modern euxinic marine basins. Geochim. Cosmochim. Acta 70, 5698–5722.

Morford, J.L., Emerson, S., 1999. The geochemistry of redox sensitive trace metals in sediments. Geochim. Cosmochim. Acta 63, 1735–1750.

Murakami, T., Sreenivas, B., Sharma, S.D., Sugimori, H., 2011. Quantification of atmospheric oxygen levels during the Paleoproterozoic using paleosol compositions and iron oxidation kinetics. Geochim. Cosmochim. Acta 75, 3982–4004.

Paulmier, A., Ruiz-Pino, D., 2009. Oxygen minimum zones (OMZs) in the modern ocean. Prog. Oceanogr. 80, 113–128.

Planavsky, N., Rouxel, O., Bekker, A., Lalonde, S.V., Konhauser, K.O., Reinhard, C.T., Lyons, T.W., 2010. The evolution of the marine phosphate reservoir. Nature 467, 1088–1090.

Planavsky, N.J., Bekker, A., Hofmann, A., Owens, J.D., Lyons, T.W., 2012. Sulfur record of rising and falling marine oxygen and sulfate levels during the Lomagundi event. Proc. Natl. Acad. Sci. USA 109, 18300–18305.

Planavsky, N.J., McGoldrick, P., Scott, C.T., Li, C., Reinhard, C.T., Kelly, A.E., Chu, X., Bekker, A., Love, G.D., Lyons, T.W., 2011. Widespread iron-rich conditions in the mid-Proterozoic ocean. Nature 477, 448–451.

Poulton, S.W., Canfield, D.E., 2011. Ferruginous conditions: a dominant feature of the Ocean through Earth's history. Elements 7, 107–112.

Poulton, S.W., Fralick, P.W., Canfield, D.E., 2004. The transition to a sulphidic ocean 1.84 billion years ago. Nature 431, 173–177.

Poulton, S.W., Fralick, P.W., Canfield, D.E., 2010. Spatial variability in oceanic redox structure 1.8 billion years ago. Nat. Geosci. 3, 486–490.

Poulton, S.W., Raiswell, R., 2002. The low-temperature geochemical cycle of iron: from continental fluxes to marine sediment deposition. Am. J. Sci. 302, 774–805.

Raiswell, R., Newton, R., Wignall, P.B., 2001. An indicator of water-column anoxia: resolution of biofacies variations in the Kimmeridge Clay (Upper Jurassic, U.K.). J. Sediment. Res. 71, 286–294.

Rasmussen, B., Buick, R., 1999. Redox state of the Archean atmosphere: evidence from detrital heavy minerals in ca. 3250–2750 Ma sandstones from the Pilbara Craton, Australia. Geology 27, 115–118.

Roscoe, S.M., Minter, W.E.L., 1993. Pyritic paleoplacer gold and uranium deposits, in: Mineral Deposit Modeling, Geological Association of Canada Special Paper 40. Geological Association of Canada, Toronto, pp. 103–124.

Rye, R., Holland, H.D., 1998. Paleosols and the evolution of atmospheric oxygen: a critical review. Am. J. Sci. 298, 621–672.

Sahoo, S.K., Planavsky, N.J., Kendall, B., Wang, X., Shi, X., Scott, C., Anbar, A.D., Lyons, T.W., Jiang, G., 2012. Ocean oxygenation in the wake of the Marinoan glaciation. Nature 489, 546–549.

Schröder, S., Bekker, A., Beukes, N.J., Strauss, H., Van Niekerk, H.S., 2008. Rise in seawater sulphate concentration associated with the Paleoproterozoic positive carbon isotope excursion: evidence from sulphate evaporites in the ~2.2–2.1 Gyr shallow-marine Lucknow Formation, South Africa. Terra Nova 20, 108–117.

Scott, C., Lyons, T.W., Bekker, A., Shen, Y., Poulton, S.W., Chu, X., Anbar, A.D., 2008. Tracing the stepwise oxygenation of the Proterozoic ocean. Nature 452, 456–459.

Shen, Y., Canfield, D.E., Knoll, A.H., 2002. Middle Proterozoic ocean chemistry: evidence from the McArthur Basin, northern Australia. Am. J. Sci. 302, 81–109.

Shen, Y., Knoll, A.H., Walter, M.R., 2003. Evidence for low sulphate and anoxia in a mid-Proterozoic marine basin. Nature 423, 632–635.

Slack, J.F., Grenne, T., Bekker, A., Rouxel, O.J., Lindberg, P.A., 2007. Suboxic deep seawater in the late Paleoproterozoic: evidence from hematitic chert and iron formation related to seafloor-hydrothermal sulfide deposits, central Arizona, USA. Earth Planet. Sci. Lett. 255, 243–256.

Sperling, E.A., Peterson, K.J., Pisani, D., 2007. Poriferan paraphyly and its implications for Precambrian palaeobiology. Geol. Soc. Lond. Spec. Publ. 286, 355–368.

Taylor, S.R., McLennan, S.M., 1985. The Continental Crust: Its Composition and Evolution. Blackwell Scientific Pub., Oxford.

Tribovillard, N., Algeo, T.J., Lyons, T., Riboulleau, A., 2006. Trace metals as paleoredox and paleoproductivity proxies: an update. Chem. Geol. 232, 12–32.

Tziperman, E., Halevy, I., Johnston, D.T., Knoll, A.H., Schrag, D.P., 2011. Biologically induced initiation of Neoproterozoic snowball-Earth events. Proc. Natl. Acad. Sci. USA 108, 15091–15096.

Van der Weijden, C.H., Middelburg, J.J., De Lange, G.J., Van der Sloot, H.A., Hoede, D., Woittiez, J.R.W., 1990. Profiles of the redox-sensitive trace elements As, Sb, V, Mo and U in the Tyro and Bannock Basins (eastern Mediterranean). Mar. Chem. 31, 171–186.

Wignall, P.B., Myers, K.J., 1988. Interpreting benthic oxygen levels in mudrocks: a new approach. Geology 16, 452–455.

Wilde, P., 1987. Model of progressive ventilation of the late Precambrian–early Paleozoic ocean. Am. J. Sci. 287, 442–459.

Zheng, Y., Anderson, R.F., van Geen, A., Fleisher, M.Q., 2002. Remobilization of authigenic uranium in marine sediments by bioturbation. Geochim. Cosmochim. Acta 66, 1759–1772.